

Apparent mass during silo discharge: Nonlinear effects related to filling protocols



Juan Pablo Peralta^a, María Alejandra Aguirre^{b,c,d}, Jean-Christophe Géminard^{c,d,e}, Luis A. Pugnaloni^{a,*}

^aDepartamento de Ingeniería Mecánica, Facultad Regional La Plata, Universidad Tecnológica Nacional, CONICET, Avenida 60 Esq. 124, La Plata 1900, Argentina

^bGrupo de Medios Porosos, Fac. de Ingeniería, Universidad de Buenos Aires, CONICET, Paseo Colón 850, Buenos Aires C1063ACV, Argentina

^cLIA PMF-FMF (Franco-Argentinian International Associated Laboratory in the Physics and Mechanics of Fluids), Argentina

^dLIA PMF-FMF (Franco-Argentinian International Associated Laboratory in the Physics and Mechanics of Fluids), France

^eUniv Lyon, ENS de Lyon, Univ Claude Bernard, CNRS, Laboratoire de Physique, Lyon F-69342, France

ARTICLE INFO

Article history:

Received 11 May 2016

Received in revised form 21 November 2016

Accepted 19 December 2016

Available online 1 February 2017

Keywords:

Granular flow

Granular discharge

Stress in silos

ABSTRACT

We study the evolution of the force exerted by a granular column on the bottom surface of a silo during its discharge. Previous to the discharge, we prepare the system using different filling procedures: *distributed*, i.e. a homogeneous rain of grains across the cross-section of the silo; *concentric*, a granular jet along the silo axis; and a combination of both, i.e. filling half of the silo using one procedure and the second half using the other. We observe that each filling protocol leads to distinctive evolutions of the apparent mass (i.e., the effective weight sensed at the base) during the discharge. Interestingly, the use of combined filling protocols may lead to a reduced apparent mass, smaller than any other achieved with a simple filling. We propose a model based on the Janssen rationale that quantitatively accounts for the latter puzzling experimental observation.

© 2017 Elsevier B.V. All rights reserved.

1. Introduction

Silos are very common structures that are broadly used to store powders or grains, i.e. granular materials. Because of the obvious importance of silos for the industry (e.g. pharmaceutical, mining, agriculture and others), questions related to the flow out of the structure through an aperture opened in the base and to the stress applied by the granular material on the walls of the structure have attracted the interest of engineers and physicists for decades.

On the one hand, when the granular material is discharged through an aperture in the base, one observes that the flow rate is constant throughout the discharge. Engineers and physicists have intensely studied the problem for the last 50 years [1–9]. Heuristically, the flow rate, W , can be shown to scale as $A^{5/2}$, where A is the size of the aperture [10–13]. This scaling, known since 1852 [9], is generally referred to as the Beverloo rule [1,14].

On the other hand, when granular material is stored in a vertical cylinder, the most remarkable feature is that the vertical stress applied by the material onto the base saturates to a constant value when the height of granular material above the base becomes large

compared to the diameter of the container. This is clearly in contrast with the pressure at the base of a viscous liquid column which increases linearly with the height of the liquid column. The effect, known as Janssen effect, is due to the fact that part of the weight of the grains is supported by the lateral walls of the container thanks to friction [9,15]. The Janssen effect has first been proposed to be at play in static conditions (in absence of flow) and reported by several authors in dedicated studies [16–20].

More recently, a screening of the weight of the grains at the bottom of a container has been observed in dynamic situations [21,22], suggesting that a dynamic Janssen-like effect can also be at play during a silo discharge. One could thus infer that the flow-rate out of a silo is constant during the discharge, independent of the height of material, because the pressure in the outlet region is constant [23]. However, measurements of the stress at the base of a discharging silo [21,24–28] and numerical studies [29] showed that the flow-rate remains constant throughout the discharge in spite of significant variation of the pressure in the outlet region.

Constitutive equations describing the stress state of granular materials during silo discharge are still lacking. In order to provide additional clues to understand the problem, we consider the effects of the filling protocol which has been shown to affect the redirection of forces towards the walls [26]. In particular, we consider the evolution of the force exerted by the grains on the bottom surface of a discharging silo for systems prepared using a combination of

* Corresponding author.

E-mail address: luis.pugnaloni@frlp.utn.edu.ar (L. Pugnaloni).

two filling protocols. We will show that some unexpected nonlinear effects are observed when two filling procedures are used. However, the use of a modified Janssen model allows us to quantitatively explain the results.

2. Experimental setup and protocols

2.1. Experimental setup

The basic idea is to measure the overall vertical force exerted on the base of a vertical silo during the discharge of granular material prepared using various protocols.

The experimental setup is similar to the one described in [21]. It consists of a silo whose vertical outer wall is a Plexiglas cylinder of internal diameter $D_c = 5$ cm, external diameter $D_e = 6$ cm and total height $H = 40$ cm (Fig. 1). At the bottom, an acrylic ring of internal diameter equal to D_c insures the mechanical contact between the cylinder and a horizontal table, such that the vertical force applied to the outer wall (its weight plus the additional force exerted by the grains) is entirely supported by the table. Inside the latter outer ring, the base of the silo consists of an acrylic disk which leans on two force sensors (KD 40S-Testwell). The outer diameter of the disk is slightly smaller than the inner diameter of the outer ring, such that the two parts are not in mechanical contact, but the gap is small enough to avoid the grains to enter therein. In this configuration, the force sensors measure the total vertical force applied to the bottom, or equivalently the apparent mass, M_{app} , of the material inside the silo. We shall report measurement of the apparent mass M_{app} during the discharge of the silo. To do so, an orifice of diameter $A = 5$ mm has been drilled at the center of the base. In order to insure a sharp edge and avoid any effect of the thickness of the disk, the orifice is slightly conical, the small diameter in contact with the grains above. During the filling procedure, the orifice is closed with a stopper which is held in place with a clamp.

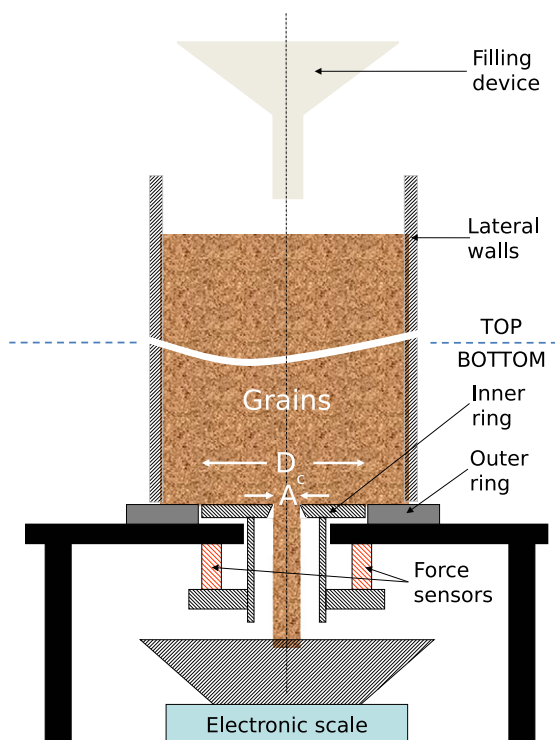


Fig. 1. Sketch of the experimental setup (see description in Section 2A).

The granular material consists of a total mass of 1 kg of glass beads ($\rho_{glass} = 2200 \text{ kg m}^{-3}$) whose diameter, d , is broadly distributed between $300 \mu\text{m}$ and $600 \mu\text{m}$.

The discharge is initiated by releasing the stopper, suddenly but without jerk thanks to the clamp. Underneath the aperture, the grains are collected in a container placed on an electronic scale. Thanks to the scale and force sensors, we measure simultaneously the discharged mass, $M(t)$, and the apparent mass, $M_{app}(t)$, as function of time, t . In what follows, for each of the experimental protocols used to prepare the system, we report data obtained for 4 to 10 experimental runs. We observed that the results are reproducible for all the protocols. The error bars correspond to the standard error of the mean, which is calculated over the independent experimental runs.

2.2. Filling procedure

In the present study, we focus on the sensitivity of the apparent mass on the way the material is prepared previous to the discharge. We therefore pay special attention to the filling procedure. We will mainly report data obtained for silos prepared in four different ways, the total initial mass of material in the silo remaining the same, equal to 1 kg:

- *Concentric (CC)*: 1 kg of granular material is poured as a jet from the top along the vertical axis of the silo using a centered funnel;
- *Distributed (DD)*: 1 kg of granular material is homogeneously deposited across the section of the silo by releasing the grains through three successive meshes [30];
- *Mixed I (CD)*: Initially, half of the total mass of grains, i.e. 500 g, is introduced in the silo using the *concentric* filling procedure; the second half of the grains being introduced using the *distributed* filling.
- *Mixed II (DC)*: Initially, half of the total mass of grains, i.e. 500 g, is introduced in the silo using the *distributed* filling procedure; the second half of the grains being introduced using the *concentric* filling.

The filling procedures lead to different initial packing fractions, even if the system is filled at the same rate. For instance, the time required to fill the silo using the *CC* and *DD* procedures are the same for our choice of funnel and meshes. However, we measure that, in average, the initial height of the granular column is $h_{CC} \cong 33$ cm for the *CC* filling whereas $h_{DD} \cong 30$ cm for the *DD* filling. The observation is compatible with previous results reported in the literature [26] showing that *DD* filled systems are denser than *CC* filled systems.

3. Experimental results

In this section, we report on the evolution of M_{app} during the discharge for systems filled with the different procedures described in Section 2.2.

We first comment that the flow-rate remains constant throughout the discharge and does not depend on the filling procedure. In addition, a convenient way to display the results consists in reporting M_{app} as function of the mass of grains, M_{in} , remaining inside the silo. The results are shown in Fig. 2. The initial mass of grains in the silo is $M_{in} = 1$ kg in all cases. Therefore, the discharge proceeds from right to left in the figure. Notice also that the final mass of grains inside the silo does not vanish since a small quantity of grains remains in a pile around the orifice at the end of the discharge.

3.1. Single filling protocols

We first focus on the results obtained for systems prepared using a single filling procedure, i.e. *concentric (CC)* or *distributed (DD)*.

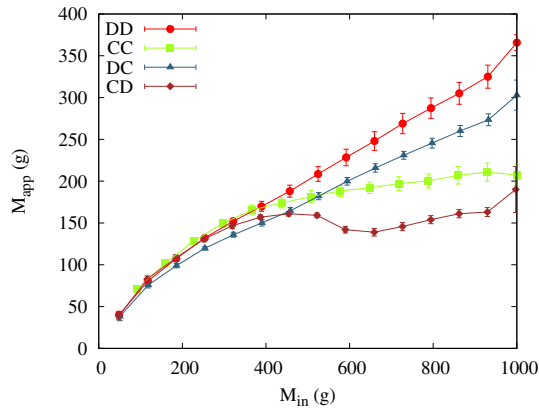


Fig. 2. Apparent mass M_{app} vs. mass M_{in} of grains inside the silo during the discharge for the different initial filling procedures described in Section 2.2: distributed (DD , red disks); concentric (CC , green squares); mixed I (CD , brown diamonds); mixed II (DC , blue triangles). The discharge proceeds from right to left. Error bars correspond to the standard error of the mean over 4 to 10 independent experimental runs. (For interpretation of the references to color in this figure legend, the reader is referred to the web version of this article.)

In the initial stages of the discharge (Fig. 2), M_{app} is considerably lower for the CC than for the DD filled systems. At first sight, this observation contradicts results by Ovarlez et al. [20], where granular systems with a higher packing fraction present a larger redirection of the granular weight to the wall, i.e. smaller M_{app} . As mentioned above, in our experimental conditions, the density achieved by the DD filling is larger than that achieved by the CC filling, which should lead to a smaller M_{app} for the DD filling, in contradiction with our experimental observations. Note however that Ovarlez et al. induce a relaxation of stresses to a steady state by slowly moving the bottom of the silo downwards by means of a vertical translational stage. In contrast, we fill the silo using different protocols that lead to different densities of the granular packing, but also to different stress distributions. It is important to realize that the packing fraction is not an indicator of how the stress is distributed in the bulk of the sample and, therefore, can not be used as a proxy for how the weight of the grains is redirected toward the walls.

The different M_{app} observed in the CC and DD filled systems can be qualitatively understood as follows. When the silo is filled using the concentric procedure, the grains initially form a pile at the center of the base. Then, as grains are added to the summit, they produce avalanches that are stopped by the lateral walls. During the filling, this dynamics creates a rather large pressure on the silo walls. In contrast, when the silo is filled using the distributed procedure, the grains fall rather uniformly across the entire cross-section of the silo and the free surface remains flat throughout the filling. The grains do not induce avalanches and one can speculate that they apply rather small normal forces on the silo walls. A large pressure on the wall leads to a large dynamic friction between the moving grains and the walls during the discharge. This qualitatively explains why the system prepared with the concentric filling has a larger portion of its weight sustained by wall friction, leading to a smaller M_{app} , in comparison with the samples prepared using the distributed filling, even if the density of the material is smaller in the concentric filling case. Vanel et al. revealed clear differences in the pressure distribution under a granular pile built with concentric and distributed procedures [17]. Note that, in our experiments, we rather focus on the differences in the pressure on the lateral wall, in the dynamical regime, during the discharge.

3.2. Mixed filling processes

Let us now discuss the results obtained for systems prepared using mixed filling procedures, i.e. concentric followed by distributed (CD) and distributed followed by concentric (DC).

We focus first on the initial stage of the discharge in Fig. 2. We observe that the apparent mass M_{app} is systematically larger when the lower half of the silo was filled using the distributed procedure, i.e. DD and DC , rather than using the concentric procedure, i.e. CC and CD . This observation can again be understood, as in Section 3.1, by considering that the redirection of the weight of the grains toward the lateral walls in the lower half is enhanced by the avalanching of the grains during the filling when the concentric (jet-like) protocol is used. We also observe that silos whose lower half is filled using the concentric procedure, i.e. CC and CD , present approximately the same M_{app} at the very beginning of the discharge. This indicates that the redirection of the weight toward the silo walls is efficient and that the lower half of the silo redirects almost entirely the mass of the upper half toward the walls. In contrast, for silos whose lower half is filled using the distributed procedure, i.e. DD and DC , the initial apparent mass depends on the filling protocol used for the upper half. For the DC filling procedure, M_{app} is smaller than for DD filling procedure. The observation is compatible with the fact that the apparent mass of the upper half supported by the lower half is smaller when the upper half is filled using the concentric procedure.

We now consider the evolution of the apparent mass throughout the discharge. We observe that the CC , DD , and DC fillings lead to monotonic dependencies of M_{app} versus M_{in} . However, the silo filled using the CD protocol has a non-monotonic behavior and M_{app} exhibits a minimum which is considerably below the apparent mass measured for the CC filling. This experimental fact is rather unexpected since a naive interpolation argument would suggest that the CD filling procedure should lead to M_{app} values in between the CC and the DD filling protocols. The result is particularly interesting when considering applications. Indeed, an unexpected small apparent mass is associated to an unexpected large pressure exerted on the lateral walls, which might be of practical importance for the design of silos.

Our experimental observations can be explained by using rather simple theoretical arguments. For instance, the very nonlinear response observed for the CD filling procedure can be explained by considering the internal rearrangements induced in the concentric lower half. However, before we go further in the analysis of the results, we propose additional experiments that provide clues to identify the relevant physical ingredients to understand the observations.

3.3. Additional experiments

In order to get further insight in the physical mechanisms that govern the apparent mass of the granular column during the discharge that is described in Section 3.2, we performed a series of complementary experiments that make possible to isolate effects like the interaction between the grains at the interface between the lower and upper half of the granular column, the friction at the wall, etc. More precisely, we analyzed the discharge of silos whose lower half was filled using either a concentric (C) or a distributed (D) procedure, completed using one of the following:

- a block of metal, having a mass of 240 g on top. This mass is similar to the apparent mass exerted by 500 g of grains filled using the distributed procedure. We denote CW (DW) for concentric (distributed) filling of the lower half with the additional weight on top (Fig. 3b).
- reduced friction of the upper half with the lateral walls. To do so, after the lower half has been filled, a cylindrical acetate film

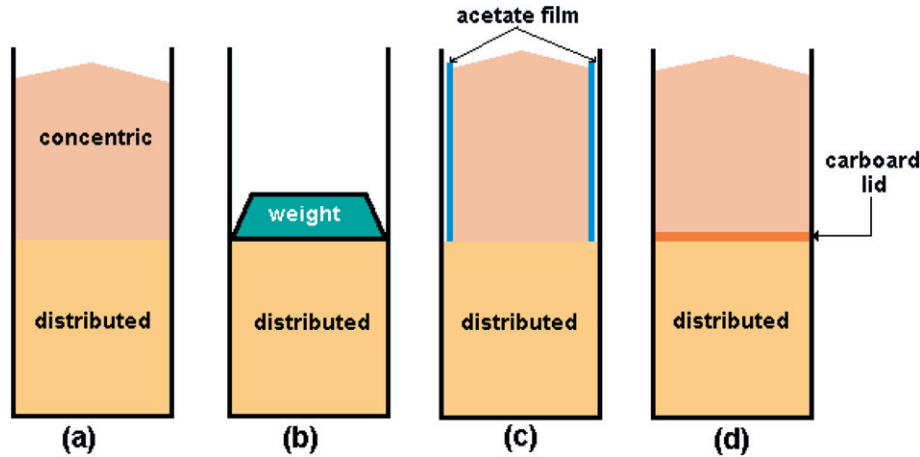


Fig. 3. Additional experimental configurations – (a) *Mixed II* (DC); (b) granular lower half plus a solid weight on top (DW); (c) reduced friction of the upper half using an acetate film (DC^0); (d) lower and upper halves separated by a cardboard disk ($D|C$).

is introduced in the silo (covering the lateral walls of the upper half) before the remaining 500 g of grains are poured in the system to fill the silo. In this case, we denote as DC^0 a *distributed* filled lower half and a *concentric* filled upper half with reduced friction (Fig. 3c). The other configurations are denoted in a similar way.

- a cardboard disk separating the lower and upper halves filled with grains. We denote as $D|C$ a *distributed* filled lower half and a *concentric* filled upper half separated by the cardboard disk (Fig. 3d). The other configurations are denoted in a similar way.

In the following Sections 3.3.1 and 3.3.2, we shall report results obtained for, respectively, *concentric* and *distributed* filling of the lower half.

3.3.1. Lower-half filled using the concentric procedure

We show in Fig. 4 the evolution of M_{app} as function of M_{in} for systems prepared as described above with the lower half filled using the *concentric* procedure. The measurements are displayed assuming a total inner mass of 1 kg even when the metallic weight is used, leading all the curves to start from $M_{in} = 1000$ g.

Let us first focus on the initial stage of the discharge in Fig. 4a. We observe that the systems prepared with the solid block (CW) and the ones with a *distributed* filling of the upper half [with ($C|D$) or without (CD) the cardboard separator] all lead to the same initial apparent mass M_{app} once the discharge is initiated. This confirms our suggestion that, initially, the upper-half filled with a *distributed* method acts as an effective overweight of about 240 g. After about 200 g of grains have been discharged, we observe in Fig. 4a that M_{app} for CW and $C|D$ preparation protocols remains larger than the apparent mass observed for the CD filling procedure. This demonstrates that preventing the direct interaction between the upper and lower half (by using the cardboard separator) has a noticeable effect.

When the wall friction is reduced in the upper part (Fig. 4b) by using the acetate film, the evolution of the apparent mass M_{app} is similar to that observed with the solid block (CW in Fig. 4a). However, in these cases (i.e., CC^0 and CD^0), due to the reduction of the friction at the lateral walls, the apparent mass M_{app} reaches a larger maximum value (of about 300 g) when the material of the lower half has been entirely discharged, i.e. for $M_{in} \approx 500$ g. It is worth mentioning here that, in Fig. 4a, M_{app} for CW and $C|D$ does not reach a maximum of 240 g due to the grains that remain in the silo after the discharge and that still partially redirect its weight toward the walls. Finally, let us comment that the *concentric* filling of the upper-half (CC) leads to a larger apparent mass than the *distributed* filling (CD), which is

quite surprising as the apparent mass of the upper half is expected to be smaller for CC . This indicates that the distribution of the stress at the interface between the lower and upper halves is such that the weight of the upper-half filled using the *distributed* procedure

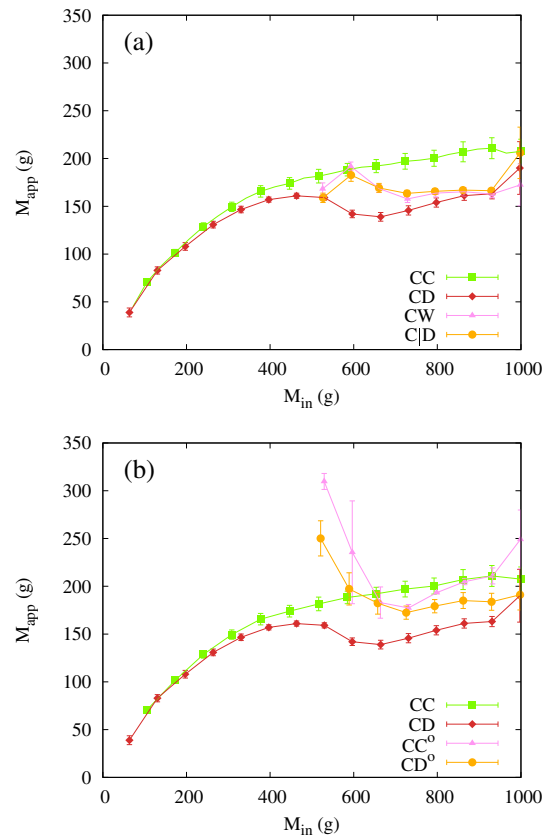


Fig. 4. Apparent mass M_{app} vs. inner mass M_{in} for silos with the lower half filled using the *concentric* procedure – (a) *concentric* (CC , green squares); mixed I (CD , brown diamonds); *concentric* lower half plus overweight on top (CW , pink triangles); mixed I with a cardboard separator ($C|D$, orange disks). (b) *concentric* (CC , green squares); mixed I (CD , brown diamonds); *concentric* (CC^0 , pink triangles) and mixed I (CD^0 , orange disks) with reduced friction at the lateral walls in the upper half. (For interpretation of the references to color in this figure legend, the reader is referred to the web version of this article.)

is somehow better redirected toward the lateral walls by the grains that are underneath.

3.3.2. Lower-half filled using the distributed procedure

In order to get further insight into the role played by the distribution of the stress at the interface between the lower and upper halves and by the friction at the lateral walls, we consider similar experiments with the lower half filled using the *distributed* procedure.

As can be observed in Fig. 5, even if the use of a *distributed* upper half (*DD*) leads to a larger apparent mass throughout the discharge, the use of the acetate film at the walls (*DC^o*) or of the cardboard separator (*D|C*) does not alter the apparent mass M_{app} as much as previously observed for the *concentric* lower half (see Section 3.3.1). This conclusion also holds when the solid block is used (*DW*). This may be due to the fact that the *distributed* filling of the lower part presents a rather flat free-surface when compared with the heap formed by the *concentric* filling.

While the reason for the lower M_{app} in *DC-* compared to *DD-* is due to the upper *concentric* half being more favorably supported by the walls, in the case of *DC^o* – where wall friction is nearly absent – the lower M_{app} is caused by an effect similar to adding a solid overweight. This induces a compression of the upper layers of the lower half that leads to an increased pressure and hence higher frictional forces on the walls, reducing the apparent mass with respect to the *DD* case.

4. Analysis and model

As mentioned in Section 3, it is quite remarkable that we measure that, as observed in Fig. 2 once the discharge is initiated, a system fully filled using the *concentric* procedure (*CC*) leads to a larger apparent mass than a system consisting of a *concentric* filling of the lower half with the upper half filled using the *distributed* procedure (*CD*). This is however compatible with the additional observation that the redirection of the weight toward the walls, and thus the screening effect, is enhanced when the pressure on the lower half due to the upper half is larger (*CD*, *CW*, *C|D* and *CD^o* in Fig. 4). Qualitatively, one can infer that an increase of the pressure at the interface leads, in a thin layer of grains below the interface, to a significant increase of the radial stress applied to the lateral walls. Thus, an enhanced dynamic Janssen-like effect during the discharge is observed. As a consequence, a smaller M_{app} is measured at the base. To model this effect, we propose a Janssen-like rationale where the different filling

protocols lead to different redirection of the forces toward the lateral walls.

4.1. Janssen rationale

In a granular column, the pressure $P(z)$ in the vertical direction, i.e. the normal component of the stress along the vertical axis, σ_{zz} , is governed by the Janssen differential equation [15]:

$$\frac{\partial P(z)}{\partial z} - \rho g + \frac{2\mu k}{R}P(z) = 0, \tag{1}$$

where z is the vertical position measured from the free surface downwards, g the acceleration of gravity, ρ the apparent density of the granular column, R the radius of the silo, μ the grain-wall friction coefficient and k the so called Janssen force-redirection factor. The latter constant factor k accounts for the proportion of the normal vertical stress transferred to the normal radial stress at the walls, i.e. $\sigma_{rr} = k \sigma_{zz}$. Usually, Eq. (1) is closed with the boundary condition $P(0) = 0$ (zero pressure at the free surface) and the well known Janssen law is obtained in the form

$$P(z) = \frac{\rho g R}{2\mu k} \left(1 - e^{-\frac{2\mu k z}{R}} \right). \tag{2}$$

From Eq. (2), the apparent mass $M_{app} = [\pi R^2 P(z)]/g$ as function of the inner mass $M_{in} = \rho \pi R^2 z$ is

$$M_{app} = M_c \left(1 - e^{-\frac{M_{in}}{M_c}} \right), \tag{3}$$

where $M_c \equiv \rho \pi R^3 / (2\mu k)$ is a characteristic mass.

As expected from Eq. (3), M_{app} indeed saturates for large values of M_{in} [see the fit of Eq. (3) to the *CC* data in Fig. 6]. The best fit to the experimental data to Eq. (3) for the *concentric* filling provides us with a measure of the characteristic mass, $M_c = (220 \pm 5)$ g, slightly smaller than in the distributed filling experiments. From the knowledge of $R = 0.025$ m, $g = 9.8$ m/s², $\rho = 1320$ kg/m³ and $M_o = 1000$ g, we estimate the product μk . Assuming further that $\mu = 0.5^1$, we get an estimate of the force-redirection factor $k = 0.31$ for the *concentric* filling (Table 1).

However, one immediately notice that Eq. (3) would fail in accounting for the dependence of M_{app} on M_{in} for the *distributed* filling procedure. Indeed, no saturation is observed (see *DD* in Fig. 6) and there is an almost linear increase of M_{app} with M_{in} .

4.2. Modified Janssen-like rationale for distributed filling

The only way to explain the linear increase of M_{app} with M_{in} for large inner mass is to consider that the redirection factor k almost vanishes for the *distributed* filling. However, some sort of screening is still at play as proven by the fact that the experimental slope of M_{app} versus M_{in} is about 1/3 (much less than unity). We thus propose that the redirection of the force toward the lateral walls is very inefficient far from the outlet, i.e. that the redirection factor k is almost zero along the column height for the *distributed* filling. However, the convergent flow of the granular material close to the outlet leads to a local redirection of the forces and, hence, the weight of the granular column is partly supported by the lateral walls in this region, only.

A convenient way to translate these ideas into a mathematical model is to write that the redirection factor takes a finite value k_o

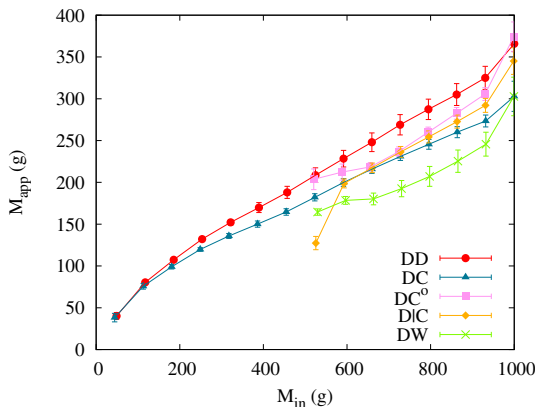


Fig. 5. Apparent mass M_{app} vs. inner mass M_{in} for lower half filled using the *distributed* procedure – *distributed* (*DD*, red disks); mixed II (*DC*, blue triangles); mixed II with reduced friction at the lateral walls in the upper half (*DC^o*, pink squares); mixed II with a cardboard separator (*D|C*, orange diamonds); *distributed* lower half plus overweight on top (*DW*, green crosses). (For interpretation of the references to color in this figure legend, the reader is referred to the web version of this article.)

¹ The value of μ is rather arbitrary. However, we use the same value in all cases (all the experiments where done with the same materials) simply to focus our discussion on k .

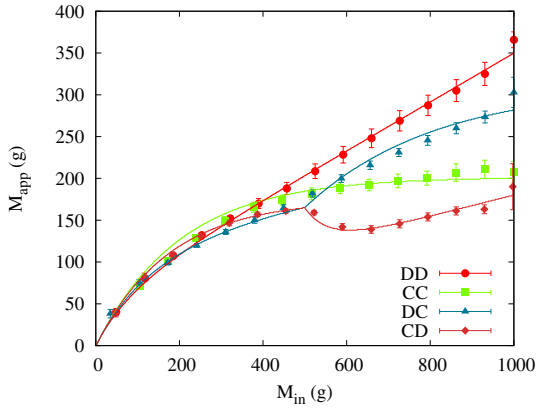


Fig. 6. Apparent mass M_{app} vs. inner mass M_{in} . The symbols are as in Fig. 2, solid lines correspond to the fits of the modified Janssen-like model.

at the base and decreases over a characteristic vertical distance \mathcal{L} above. We thus write

$$k(z) = k_0 \exp(-z/\mathcal{L}). \quad (4)$$

In this picture, the distance \mathcal{L} is governed by the geometry and one expects it to be of the order of the container diameter $2R$.

Following a Janssen-like rationale, we write, for the pressure along the vertical direction

$$\frac{\partial P(z)}{\partial z} - \rho g + \frac{2\mu k_0}{R} \exp(-z/\mathcal{L}) P(z) = 0, \quad (5)$$

The solution of Eq. (5), with the additional boundary condition that $P = 0$ at the free surface, leads to

$$M_{app} = M_c \left(\tilde{L} e^{-\tilde{L}} \right) \left[E_i(\tilde{L}) - E_i\left(\tilde{L} e^{-\frac{M_{in}}{M_c}} \right) \right], \quad (6)$$

where we introduced the reduced length $\tilde{L} \equiv 2k_0\mu\mathcal{L}/R$ and the characteristic mass $M_c \equiv \rho\pi R^3/(2\mu k_0)$ defined using k_0 . The function $E_i(x)$ is the exponential integral given by $E_i(x) \equiv -\int_{-x}^{\infty} \frac{e^{-u}}{u} du$. Equation (6) predicts, after a transient, the linear increase of M_{app} as a function of M_{in} with a slope smaller than unity. The best fit of the experimental data for the DD filling in Fig. 6 using Eq. (6) leads to estimates of both the redirection factor $k_0 \simeq 0.7$ and the characteristic length $\mathcal{L} \simeq 4.4$ cm (Table 1). Note that this latter value is, as expected if the model is correct, similar to the container diameter. Note also that the redirection factor k_0 corresponds to a reasonable angle of redirection of $\tan^{-1}(0.7) \approx 35^\circ$ (this is about the angle of repose of the pile that remains at rest around the outlet at the end of the discharge)

Our Janssen-like rationale accounts thus correctly for the measurements of the apparent mass in the case of a simple distributed filling. In the next section, we show that the combination of a Janssen

screening effect, with a constant value of k for the concentric filling (Section 4.1) and a “short-ranged” $k(z)$ for the distributed filling (Section 4.2) accounts for the experimental measurements of the apparent mass when a mixed procedure is used.

4.3. Mixed filling procedure

We considered granular silos consisting of two halves, prepared in different ways. When solving Eq. (1) for a lower half filled using the concentric procedure or Eq. (5) for a lower half filled using the distributed procedure, one must thus consider as boundary condition, at the interface separating the two parts of the system, the pressure resulting from the upper part of the column of grains, instead of $P = 0$.

For a lower half filled using the concentric procedure, the solution of Eq. (1) with the condition that $P(h_{lo}) = P_0$, where h_{lo} denotes the height of the lower part of the column (which decreases during the discharge) and P_0 the pressure resulting from the grains of the upper half that lean on top, leads to

$$M_{app} = M_c \left(1 - e^{-\frac{2M_{in}-M_0}{2M_c}} \right) + M_{app}^{up} e^{-\frac{2M_{in}-M_0}{2M_c}}. \quad (7)$$

We have taken into account that the height, h_{lo} of the lower part is a function of the inner mass according to $\rho\pi R^2 h_{lo} = M_{in} - M_0/2$ where M_0 is the initial total mass on grains poured in the silo. The relation holds true as long as $M_{in} > M_0/2$, i.e. while there remain grains of the lower half in the silo. In Eq. (7), M_{app}^{up} is the apparent mass of the upper half estimated at the interface. For an upper half prepared with a distributed filling, M_{app}^{up} is given by Eq. (6) with $M_{in} = M_0/2$. This is because the total mass of grains in the upper half remains constant and equal to $M_0/2$ during the first half of the discharge (i.e. while $M_{in} > M_0/2$). The second half of the discharge ($M_{in} < M_0/2$) is then described by Eq. (6) when the grains of the upper part, filled using the distributed protocol, are flowing out of the silo. The best fit to the experimental data reported for the CD filling in Fig. 6 to Eqs. (6) and (7) leads to the redirection factor $k \simeq 0.37$ for the concentric half and to the redirection factor $k_0 \simeq 0.67$ and the characteristic length $\mathcal{L} = 7.7$ cm for the distributed half. These values, reported in Table 1, will be discussed below.

Finally, for a lower half filled using the distributed procedure, we can solve, in a similar way, Eq. (5) with the condition that $P(h_b) = P_0$, where h_b denotes the height of the lower part of the column, the pressure P_0 resulting from the apparent mass of the upper half, filled using the concentric protocol, which is given by Eq. (3) with $M_{in} = M_0/2$ during the first half of the discharge. The best fit of the experimental data reported for the DC filling in Fig. 6 to the model leads to the redirection factor $k \simeq 0.21$ for the concentric filling and to the redirection factor $k_0 \simeq 0.60$ and the characteristic length $\mathcal{L} = 7.5$ cm for the distributed filling (Table 1). We can see that, in spite of the experimental scatter, k , k_0 and \mathcal{L} remain of the same order in all the experimental conditions used in our study.

We first comment on the values of the redirection factor, k , measured for the concentric filling. For the CC filling we measured $k \simeq 0.31$ whereas k is found slightly larger ($k = 0.37$) for a concentric bottom half underneath a distributed upper half and significantly smaller ($k = 0.21$) when the concentric half is on top of a distributed lower half. For the CD filling, the filling procedure is interrupted before the grains are poured as a rain on top. It might be that the mechanical perturbations associated to the manipulation have the effect of a slight tapping of the system, which might result in a more efficient redirection of the force toward the lateral walls (larger k), as it is observed when adding a solid overweight. For the DC filling, the discharge of the material underneath is likely to disorganize the texture of the concentric upper half, leading to a lower efficiency of the redirection toward the walls (smaller k).

Table 1

Experimental redirection factor, k , (for concentrically filled part of the column) and characteristic redirection, k_0 , and characteristic length, \mathcal{L} , (for the distributed filled part of the column) in the four different filling protocols.

		CC	DD	CD	DC
C-filled part	k	0.31	–	0.37	0.21
D-filled part	k_0	–	0.70	0.67	0.60
	\mathcal{L} (cm)	–	4.4	7.7	7.5

Let us now focus on the value of the redirection factor, k_0 , and of the characteristic length, \mathcal{L} , measured for the *distributed* filling. We remind that we considered that the redirection of the force toward the lateral walls is induced by the geometry of the convergent flow at the lower region of the column of grains. For the *DD* and *DC* fillings, the pile of steady grains that surround the outlet might redirect the force toward the walls and we estimated from the measured values of k_0 that they correspond to a typical angle of about 35° , compatible with the typical angle of avalanche. We remark that for the *CD* filling, the *concentric* lower-half initially screens out the contribution of the *distributed* upper-half. Thus, the redirection factor k_0 for the *distributed* upper-half plays an important role only when the first half has been discharged and when the material of the upper-half enters in contact with the bottom. It is thus likely that, when the upper half filled using the *distributed* protocol reaches the bottom of the container, the same reasoning holds and the value of k_0 must be of the same order in this case. We indeed measure that k_0 remains around 0.7 in all the configurations. Concerning the characteristic length, the values of \mathcal{L} for the *DD* and *DC* fillings are expected to be of the same order because the material of the bottom is confined in the same geometry. It is more surprising, at first sight, to get almost the same for the *CD* filling, for which the *distributed* upper-half sits on the lower half and not on the solid bottom. But, again, the redirection for the *distributed* upper-half is expected to play an important role only when the first half has been discharged and when the material of the upper-half enters in contact with the bottom. In this case, the geometrical conditions are the same. We notice, however, a factor of two in the characteristic length \mathcal{L} , but, considering that the model is crude, the characteristic length remains of the order of the container diameter.

5. Discussion and conclusions

We assessed, during the discharge, the evolution of the apparent mass of the grains measured at the base of a vertical silo. We observed that M_{app} versus M_{in} depends drastically on the protocol used to fill the system. We considered silos filled in part using a *concentric* and in part using a *distributed* protocol.

In all cases, a large portion of the weight of the grains is supported by the lateral walls. We observe that the redirection of the weight toward the walls is more efficient for the *concentric* than for the *distributed* filling protocols. For the *concentric* protocol, the redirection is so efficient that it leads to the saturation of the apparent mass when the height of the granular column is increased. In contrast, for the *distributed* protocol, the redirection is so inefficient that the apparent mass does not saturate when the height of the granular column is increased. From the theoretical analysis, we conclude that, for the *distributed* filling, about 1/3 of the weight is supported by the base of the silo, whereas the remaining part (about 2/3) of the weight is supported by friction over a small lower region of the wall whose height compares to the diameter of the silo. This implies that the grains exert a large normal stress onto the lateral walls only in this region for the *distributed* filling protocol.

We also found that filling the silo in two stages, half with *concentric* filling and half with *distributed* filling, leads to a nonlinear, non-monotonic evolution of M_{app} as a function of M_{in} . If the lower half corresponds to the *concentric* filling procedure, the system keeps memory of the filling history and shows a marked change in the pressure trend when the second half of material (filled with the *distributed* procedure) starts evacuating. In addition, we observed that filling the container using two successive different protocols can lead to an apparent mass smaller than that achieved using any of the single filling protocols. This means that the lateral walls sustain larger stresses than those obtained with just one filling protocol.

We have shown that a Janssen-like model can be used to quantitatively explain the experimental results and to predict the apparent masses for the still little explored cases of *distributed* filling and mixed filling protocols.

These findings are of particular importance when designing operational protocols for filling and emptying silos, since the stress on walls can be largely affected and the system can keep memory of the history of the filling procedures even after significant manipulation. The larger the forces at the wall, the larger their wear and possible collapse [31]. Since it is generally simpler and more affordable to reinforce the base of a silo, a *distributed* filling protocol—which showed the higher M_{app} —should be considered of preference over a *concentric* filling. However, one must consider to reinforce not only the bottom but also the lower part of the lateral walls in a region extending vertically over typically a silo diameter.

It is also important to mention that changes in the filling protocols must be considered with some care to avoid compromising a silo structure. If a silo usually filled *concentrically* is completed using a *distributed* procedure—without emptying the remaining of previous *concentrically* filled material—the walls may initially suffer a larger stress than keeping the usual *concentric* filling.

Acknowledgments

We thank M. E. Fernández for help with some of the experiments. This work has been supported by the ANPCyT (Argentina) through grant PICT-2012-2155, and the Centro Argentino Francés de Ciencias de la Ingeniería (CAFCI, CONICET-CNRS) through grant R147-15.

References

- [1] W.A. Beverloo, H.A. Leninger, J. van de Valde, Chem. Eng., Sci. 15 (1961) 260.
- [2] L.P. Kadanoff, Rev. Mod. Phys. 71 (1999) 435.
- [3] P.G. de Gennes, Rev. Mod. Phys. 71 (S374). (1999).
- [4] V. Trappe, V. Prasad, L. Cipelletti, P.N. Serge, D.A. Weitz, Nature 411 (London) (2001) 772.
- [5] H.M. Jaeger, S.R. Nagel, R.P. Behringer, Rev. Mod. Phys. 68 (1996) 1259.
- [6] J. Duran, Sands, Powders and Grains, Springer, New York, 2000.
- [7] G.H. Ristow, Pattern Formation in Granular Materials, Springer, New York, 2000.
- [8] S.B. Savage, R.M. Nedderman, U. Tüzün, G.T. Houlsby, J. Chem. Eng. Sci. 38 (1983) 189–195.
- [9] G.H.L. Hagen, Berlin, bericht über die zur bekanntmachung geeigneten verhandlungen der königlich preussischen akademie der wissenschaften zu berlin, 35 (1852) 35–42. (Translation and comments).
- [10] B.P. Tighe, M. Sperl, Berlin, bericht über die zur bekanntmachung geeigneten verhandlungen der königlich preussischen akademie der wissenschaften zu berlin, Granul. Matter 9 (2007) 141–144. (Translation and comments).
- [11] R.M. Nedderman, Laohakul, C. 25 (1980) 91–100.
- [12] J.Y. Zhang, V. Rudolph, Ind. Eng. Chem. Res 30 (1991) 1977–1981.
- [13] C. Mankoc, A. Janda, R. Arévalo, J.M. Pastor, I. Zuriguel, A. Garcimartín, D. Maza, Gran. Matter 9 (2007) 407–414.
- [14] H. Sheldon, D.J. Durian, Granular. Matter. 12 (2010) 579–585.
- [15] R.L. Brown, J.C. Richards, Principles of Powder Mechanics, Pergamon Press, Oxford, 1970.
- [16] H.A. Janssen, Zeitung des vereins deutscher ingenieure, 39 (1895) 1045. (Translation and comments).
- [17] M. Sperl, Zeitung des vereins deutscher ingenieure, Granul. Matter 8 (2006) 59–65. (Translation and comments).
- [18] L. Vanel, E. Clément, Eur. Phys. J. B 11 (1999) 525–533.
- [19] L. Vanel, D. Howell, D. Clark, R.P. Behringer, E. Clément, Phys. Rev. E 60 (1999) R5040.
- [20] E. Kolb, T. Mazozi, E. Clément, J. Duran, Eur. Phys. J. B 8 (1999) 483–491.
- [21] L. Vanel, P. h. Claudin, J.P.h. Bouchaud, M.E. Cates, E. Clément, J.P. Wittmer, Phys. Rev. Lett. 84 (7) (2000) 1439–1442.
- [22] G. Ovarlez, C. Fond, E. Clement, Phys. Rev. E. 67 (060302 R). (2003).
- [23] C. Perge, M.A. Aguirre, P.A. Gago, L. Pugnaloni, D. Le Tourneau, J.C. Géminard, Phys. Rev. E. 85 (2012) 021303.
- [24] Y. Bertho, F. Giorgiutti-Dauphiné, J.-P. Hulin, Phys. Rev. Lett. 90 (2003).
- [25] See for example R.L. Brown, J.C. Richards, Trans. Inst. Chem. Eng. 38 (1960) 243–256. (comment on pp.167).
- [26] See for example H.M. Jaeger, S.R. Nagel, Science 260, 255 (5051) (1992) 1523–1531. (comment on pp.1527).

- See for example H.M. Jaeger, S.R. Nagel, R.P. Behringer, *Rev. Mod. Phys.* 68 (5051) (1996) 1259–1273. (comment on pp.1261).
- See for example J. Kakalios, *Am. J. Phys.* 73 (1) (2005) 8–22. (comment on pp.15).
- See for example C.S. Campbell, *Powder Technol.* 162 (1) (2006) 208–229. (comment on pp.212).
- [24] M.A. Aguirre, J.G. Grande, A. Calvo, L.A. Pughaloni, J.C. Géminard, *Phys. Rev. Lett.* 104 (2010) 238002.
- [25] M.A. Aguirre, J.G. Grande, A. Calvo, L.A. Pughaloni, J.C. Géminard, *Phys. Rev. E.* 83 (2011) 061305.
- [26] Z. Zhong, J.Y. Ooi, J.M. Rotter, *Eng. Struct.* 23 (2001) 756–767.
- [27] H.J. Pacheco-Martinez, J.C. van Gerner, H. Ruiz-Suárez, *Phys. Rev. E.* 77 (2008) 021303.
- [28] H. Ahn, Z. Başaranoğlu, M. Yilmaz, A. Buğutekin, M. Zafer Gül, *Powder Technol.* 186 (2008) 65–71.
- [29] L. Staron, P.Y. Lagrée, S. Popinet, *Phys. Fluids*, 24 (10) (2012) 113303.
- [30] The three stainless steel meshes are spaced in a cylindrical frame of 50mm in height and 38mm in diameter. Each mesh has 16×12 wires per inch.
- [31] G. Gutiérrez, C. Colonnello, P. Boltenhagen, J.R. Darias, R. Peralta-Fabi, F. Brau, E. Clément, *Phys. Rev. Lett.* 114 (2015) 018001.